Available online at www.synsint.com

Synthesis and Sintering

ISSN 2564-0186 (Print), **ISSN** 2564-0194 (Online)

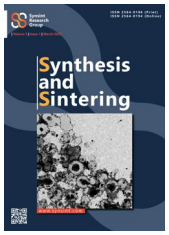

Research article

Characterization of hot-pressed biodegradable zinc-based nanocomposite implant materials reinforced with 10 wt% Mg, WE43, and AZ91

Onur Fevzi Kevenlik [a,*], **Shanli Salahi** [b,*], **Yiğit Yalçın** [b], **Hanifi Çinici** [b], **Recep Çalın** [c]

[a] *Department of Defense Technologies, Kırıkkale University, 71450, Kırıkkale, Turkey*
[b] *Department of Metallurgical and Materials Engineering, Gazi University, 06500, Ankara, Turkey*
[c] *Department of Metallurgical and Materials Engineering, Kırıkkale University, 71450, Kırıkkale, Turkey*

A B S T R A C T

Compared to permanent orthopedic implants for load-bearing applications, biodegradable implants eliminate the necessity for surgical removal after the healing process. Furthermore, magnesium alloy powder reinforced zinc matrix implant materials have been produced to enhance the mechanical properties, biocompatibility, and a proper degradation rate with the growth rate of new bones. This study aims to fabricate Zn-10 wt% Mg, Zn-10 wt% WE43, Zn-10 wt% AZ91, and alloys along with pure Zn sample for control, using the powder metallurgy production method. In this context, hot pressing was applied to samples at 200 °C and 300 °C temperatures, under a constant pressure of 400 MPa to optimize the fabrication parameters. Scanning Electron Microscope (SEM), Energy Dispersive Spectrometry (EDS), Vickers macro- and micro-hardness test (HV), and X-Ray Diffraction Spectroscopy (XRD) analyses were performed to investigate the influence of press temperatures on the microstructure, elemental components, and mechanical properties of the fabricated samples. The microstructures of the zinc matrix nanocomposite samples reinforced with magnesium alloys predominantly consist of $MgZn_2$, Mg_2Zn_{11}, and MgO phases dispersed within the refined zinc matrix. The obtained results indicate that Zn – Mg alloy nanocomposites hold significant potential as biodegradable orthopedic implant materials; however, it is possible to further improve the properties of the material by optimizing the production parameters.

KEYWORDS

Zn-Mg alloy
Nanocomposite
Powder metallurgy
Biodegradability
Mechanical properties

OPEN ACCESS

1. Introduction

Biodegradable implants provide crucial advantages in load-bearing applications compared to conventional permanent implant materials. Biodegradable implants are engineered to gradually self-degrade once their supporting functions in the human body cease. This self-dissolving advantage negates the need for additional surgical intervention to remove the implant material, thereby reducing healthcare costs and minimizing the patient's post-operative recovery period [1–4]. As the global population ages, the demand for surgical reconstruction increases, creating a significant need for implant materials in surgical procedures. For instance, in the United States alone, approximately 100,000 anterior cruciate ligament (ACL) repair surgeries are performed annually [5]. Addressing this situation requires

* Corresponding authors. *E-mail address:* 208867004@kku.edu.tr (O.F. Kevenlik), shanli.salahi@gazi.edu.tr (S. Salahi)
Received 31 January 2025; Received in revised form 9 March 2025; Accepted 9 March 2025.

https://doi.org/10.53063/synsint.2025.51269

increased research and innovation projects aimed at the design and development of next generation biodegradable implant materials. Among various material's categories, biodegradable metallic materials are considered by researchers to be more suitable materials for implant applications, owing to their superior mechanical properties compared to polymeric alternatives.

Zinc is a crucial element, which has a vital function within the human body and is considered as one of the fundamental demanded components for human physiological processes [6]. This element is extensively distributed in body tissues, with approximately 85% found in muscle and bone, 11% is found in skin and liver, and the remaining portion is presented throughout the other tissues. In multicellular organisms, roughly 30–40% of the zinc element is stored in the nucleus, 50% is stored within the cytoplasm, organelles and special vesicles (such as those in digestive enzymes or hormone storage domain), while 10–20% are remnants in the cell membrane. Due to the important functions of zinc within the human body, the recommended daily consumption amount has been determined as 15 mg [7]. Additionally, zinc plays a critical role in the human body, being a vital constituent of many enzymes and proteins. The risk of zinc poisoning is extremely rare, considering its LD50 is 27 g/day. However, since the vomiting threshold is around 225–400 mg/day, ingestion of this amount is practically impossible. Zinc deficiency within the human body negatively affects growth, neuronal development, immune function, protein and DNA synthesis, wound healing, and many other vital biological processes [8, 9]. Considering the evaluations described, zinc is suggested to be a promising biodegradable material, leading to intensive research focused on developing the zinc-based biodegradable composite implant materials [10–16].

Zinc (Zn) and magnesium (Mg) have become as key focal point among various biodegradable metallic materials due to their critical roles in numerous biological functions and their biocompatibility characteristics [17, 18]. A major challenge associated with magnesium is its high susceptibility to corrosion, which occurs as a result of the rapid biological degradation process in the human body. The resulting rapid corrosion can lead to a deterioration of the implant material's mechanical integrity during the tissue healing process. Moreover, the corrosion rates of magnesium and its alloys can cause accelerated hydrogen evolution and alkalinization of body fluids, thus potentially adversely affecting homeostatic mechanisms and impeding the tissue healing process and leading to additional challenges of implant's biomedical applications [19–21]. Recent research has shown that zinc, being a more noble metal compared to magnesium, offers substantially higher corrosion resistance behavior without compromising both its mechanical integrity and biocompatibility characteristics [8, 12, 22].

The main limitations of pure zinc, as a biodegradable metallic material for implants production, are its low mechanical strength and plasticity. The tensile strength of cast zinc is less than 20 MPa and the strain value is 0.2% [8]. To improve the pure Zinc's mechanical properties, the alloying method is often preferred. The additive powder materials used in the alloying method play a crucial role in bone formation, mineralization and numerous enzymatic reactions occurring in the human body. Especially magnesium and its alloys (WE43 and AZ91) stand out as promising candidates for such biomedical applications. Many new magnesium alloys have been developed to solve the rapid corrosion problem of pure magnesium material. Regarding this context Mg, WE43, and AZ91 alloys have emerged as suitable candidates for implant material production due to their adequate mechanical properties and lower corrosion rates compared to the most other magnesium alloys. The demanded biodegradable implant material's properties are improved by reinforcing the matrix material with WE43 and AZ91 powders, thus the additive alloys increase the potential of zinc-based biodegradable implant material to provide mechanical support during tissue healing processes. Furthermore, superior mechanical properties can be imparted to the samples by applying sintering heat treatment in addition to thermal deformation production method such as powder metallurgy [23–27].

This research article aims to design a zinc-based biodegradable implant material with enhanced mechanical characteristics by the powder metallurgy production method. Three groups of samples that contain 10 wt% magnesium alloy powder (Mg, WE43, and AZ91) reinforced zinc matrix biodegradable nanocomposite material were produced. To optimize the production parameters, the effect of temperature on the mechanical properties of the material was investigated by hot pressing the samples at 400 MPa pressure under the temperatures of 200 °C and 300 °C for determining ideal production conditions.

2. Materials and methods

The Zn powder used as the matrix of the implant nanocomposite material has a purity of 99% and a powder size of <45 μm, supplied by TMC Powder Metal company. Reinforcement powders are pressed samples produced by powder metallurgy method using pure Mg powders with grain size of <63 μm, AZ91 magnesium alloy powders with particle size of <150 μm (composition by weight %, Al: 8.77; Zn: 0.74; Ni <0.01; Cu <0.01 and the remnant is Mg) supplied by Zhejiang Bainianyin Industry and Trade Company, and WE43 magnesium alloy powders with particle size of <45 μm (composition by weight %, Y: 3.7–4.3; Zr: 0.4–1; Nd: 2–2.5; Gd: 0.1–1.9 and the remnant is Mg) supplied by Magnesium Elektron® Ltd.

Regarding the powders preparation step, Mg, WE43, and AZ91 powders were added to the samples at a 10 wt% ratio. The powder mixtures were initially homogenized in a turbula mixer for 1 hour. Sample production was carried out using a specially designed single-axis, 200 ton capacity hydraulic press device, which was used to press the samples at temperatures of 200 °C and 300 °C under the constant pressure of 400 MPa.

In order to evaluate the mechanical properties of the fabricated samples, density analysis was conducted using WSA-224T instrument

Table 1. Codes and production parameters of Zn-based nanocomposite samples fabricated by powder metallurgy method.

Sample code	Production parameters		
	Component (wt%)	Pressure (Mpa)	Temperature (°C)
A43	Pure Zn	400	300
BL42	10 Mg	400	200
BL43	10 Mg	400	300
DL42	10 WE43	400	200
DL43	10 WE43	400	300
CL42	10 AZ91	400	200
CL43	10 AZ91	400	300

A43
Pure Zn
400 MPa
300°C

Element Number	Element Symbol	Element Name	Atomic Conc.	Weight Conc.
6	C	Carbon	14.685	3.600
8	O	Oxygen	17.147	5.600
12	Mg	Magnesium	0.201	0.100
30	Zn	Zinc	67.966	90.700

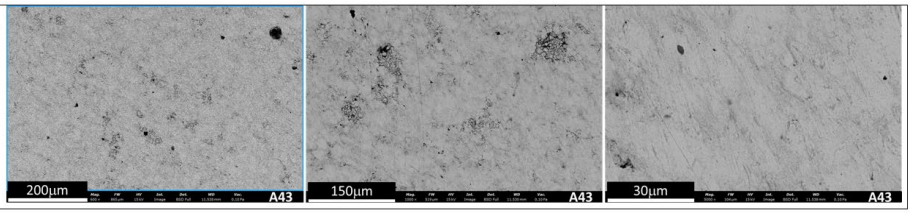

Fig. 1. The SEM micrographs and EDS analyses results of the pure Zn reference sample, which coded as A43 and produced by powder metallurgy method.

in both air and water conditions. Furthermore, HV5 macro- and HV0.3 micro-hardness analyses were conducted using Emcotest Duravision 200 and Shimadzu HMV-2 instruments under the loads of 5 kg and 300 g, respectively. Through the characterization phase, density, macro-hardness and micro-hardness measurements, and the microstructural and compositional characterization of the nanocomposite materials were performed and analyzed.

3. Results and discussion

3.1. Microstructural and compositional characterization

The microstructural and elemental composition analyses of the pure Zn control sample, A43, that was produced by powder metallurgy method at a temperature of 300 °C under a constant pressure of 400 MPa, were examined using Scanning electron microscope (SEM) and Energy dispersive x-ray spectroscopy (EDS) and are presented in Fig. 1.

Moreover, the SEM micrographs and EDS analyses results for 10 wt% Mg reinforced Zn matrix nanocomposite demonstrated in Fig. 2. The EDS analysis revealed the significant changes in the phase elemental concentration of the samples reinforced with 10 wt% Mg, coded as BL42 and BL43, which were subjected to hot pressing at 200 °C and 300 °C variable temperature parameters, respectively, under a constant pressure factor of 400 MPa. As a result of hot pressing at 200 °C, intermetallics and phases such as $MgZn_2$, Mg_2Zn_{11}, and MgO [28–31] nucleate and initiate to grow as relatively homogeneous and fine-grained precipitates within α-Zn matrix, thus the intermetallics coarsen as a result of diffusion-driven growth due to the increase in the pressing temperature to 300 °C. The growth of intermetallics is encouraged due to the increased diffusion as a result of the rise in the pressing temperature; however, it simultaneously induces phase separation, thermal distortion and the formation of micro-cracks specifically along grain boundaries, as evident in the SEM micrographs.

Fig. 3 indicates the SEM micrographs and EDS analysis results of the 10 wt% WE43 reinforced Zn matrix nanocomposite samples, coded as DL42 and DL43, which were hot pressed at 200 °C and 300 °C temperature and fabricated under 400 MPa constant pressure. The increase in pressing temperature from 200 °C to 300 °C significantly affects the distribution and recrystallization of $MgZn_2$, Mg_2Zn_{11} intermetallics and MgO phase [28–32] in the α-Zn matrix as shown in the SEM micrographs of the nanocomposite samples. The elevated temperature enhances the diffusion of magnesium into the zinc matrix, leading to the formation of coarser-grained $MgZn_2$, Mg_2Zn_{11} intermetallic phases, alongside with more distinct phase boundaries between the phases. Additionally, the oxygen concentration increases from 13.34% in DL42 to 28.44% in DL43, indicating enhanced oxidation and MgO formation at 300 °C hot pressing temperature.

The EDS analysis of the 10 wt% AZ91 reinforced nanocomposite sample, coded as CL42, hot pressed at 200 °C under 400 MPa pressure, revealed moderate oxygen content (20.80%) promoted the formation of a homogeneously distributed MgO phase within the α-Zn matrix. The presence of MgO indicates that limited diffusion occurred at the low pressing temperature. Upon reaching the pressing temperature of 300 °C during the production of the CL43 sample, it was observed that enhanced diffusion led to a higher oxygen concentration (28.93%) and a corresponding decrease in magnesium content, increasing in MgO phases. The SEM micrographs indicate the growth of $MgZn_2$ and

BL42
%10 Mg
400 MPa
200°C

Element Number	Element Symbol	Element Name	Atomic Conc.	Weight Conc.
6	C	Carbon	6.846	2.400
8	O	Oxygen	14.987	7.000
12	Mg	Magnesium	48.878	34.700
30	Zn	Zinc	29.289	55.900

BL43
%10 Mg
400 MPa
300°C

Element Number	Element Symbol	Element Name	Atomic Conc.	Weight Conc.
6	C	Carbon	10.973	4.296
8	O	Oxygen	15.133	7.892
12	Mg	Magnesium	52.048	41.259
30	Zn	Zinc	21.845	46.553

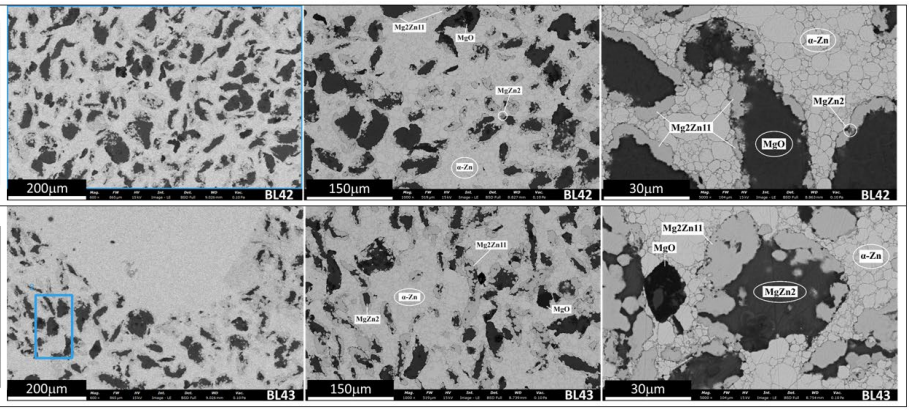

Fig. 2. The SEM micrographs and EDS analysis results of BL42 and BL43 samples with 10 wt% Mg content.

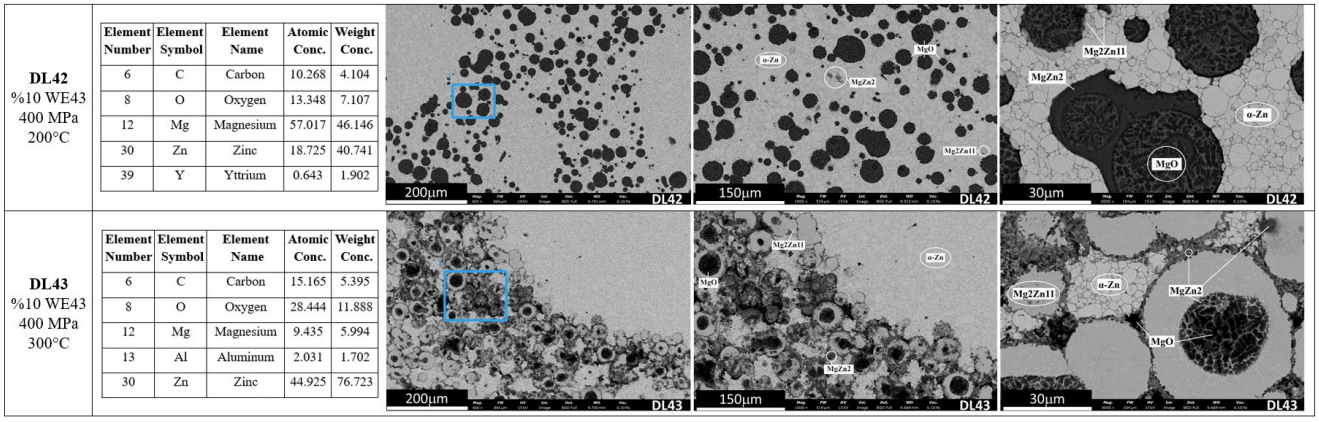

Fig. 3. The SEM micrographs and EDS analysis results of DL42 and DL43 samples reinforced with 10 wt% WE43 magnesium alloys powder.

Mg_2Zn_{11} intermetallics [28–31,33] along the α-Zn matrix due to the elevated temperature. Additionally, macro- and micro-cracks were detected due to the increased intragranular stress concentration (Fig. 4). The general conclusion obtained from the SEM microstructures of the Zn-based nanocomposites indicates that the addition of pure Mg powder to the matrix results in various-shaped intermetallics. The WE43 reinforced nanocomposites demonstrate spherical intermetallics; however, the AZ91 reinforced nanocomposites exhibit a lamellar microstructure. It's important to note that the presence of carbon element in the EDS analyses of the samples is due to the bakelite material used in embedding the samples to ensure the stability of the samples during the metallography sample preparation and characterization stages, respectively.

3.2. Mechanical characterization

In this research paper, the standard Archimedes method was utilized to determine the density and the porosity of the reinforced Zn-based nanocomposites produced by the powder metallurgy method. Moreover, the density, porosity, and Vickers hardness values of fabricated samples are provided in Fig. 5.

The pure Zn sample, A43, which was hot pressed at 300 °C under 400 MPA pressure, exhibited the highest density of 92.16% with a low porosity of 7.84%, thus it was observed that the sample had a compact structure. In contrast to the A43 sample, the BL43 sample that reinforced with 10 wt% pure Mg powder and sintered after hot pressing procedure at 400 MPA and 300 °C indicated a minimum density value of 73.21% with a maximum porosity structure of 26.80%.

Vickers HV5 macro- and HV0.3 micro-hardness values explained the structural differences in the produced nanocomposite samples. While the HV0.3 micro-hardness values of the nanocomposite samples varied in the range of 52.9–72.4, the HV5 macro-hardness values were in the range of 53.5–73.0 [28, 34, 35]. Notably, the increased porosity of low density samples such as BL43 and DL42 caused them to exhibit lower hardness values. This characteristic behavior suggests that increased structural porosity reduces the integrity of the implant material, resulting in lower mechanical properties. The established correlation between porosity and hardness properties of hot-pressed samples by powder metallurgy method provides the basis for optimizing density, porosity and hardness of nanocomposite implant samples for their intended use by emphasizing the effect of microstructural properties on the mechanical performance of the fabricated material.

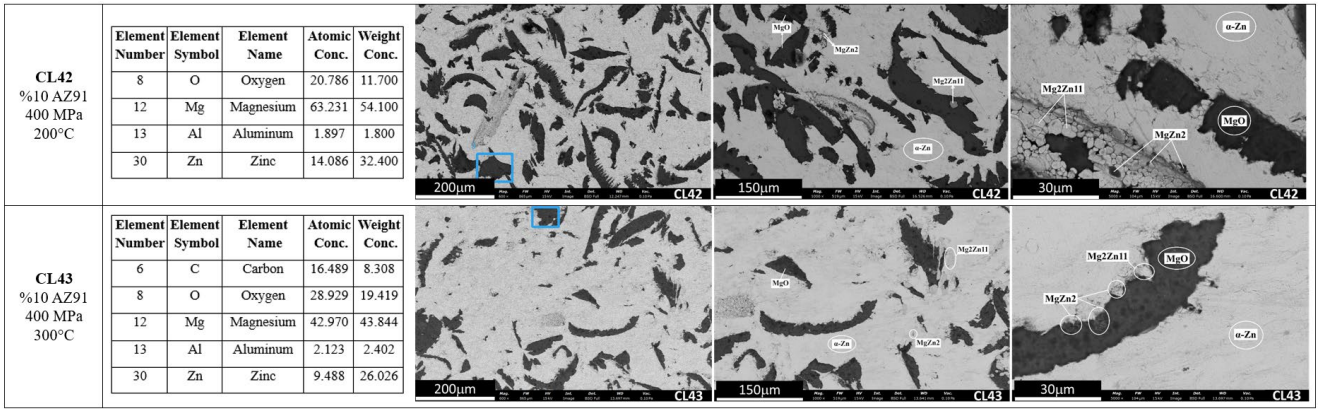

Fig. 4. The SEM micrographs and EDS analysis results of CL42 and CL43 samples containing 10 wt% AZ91 magnesium alloys powder.

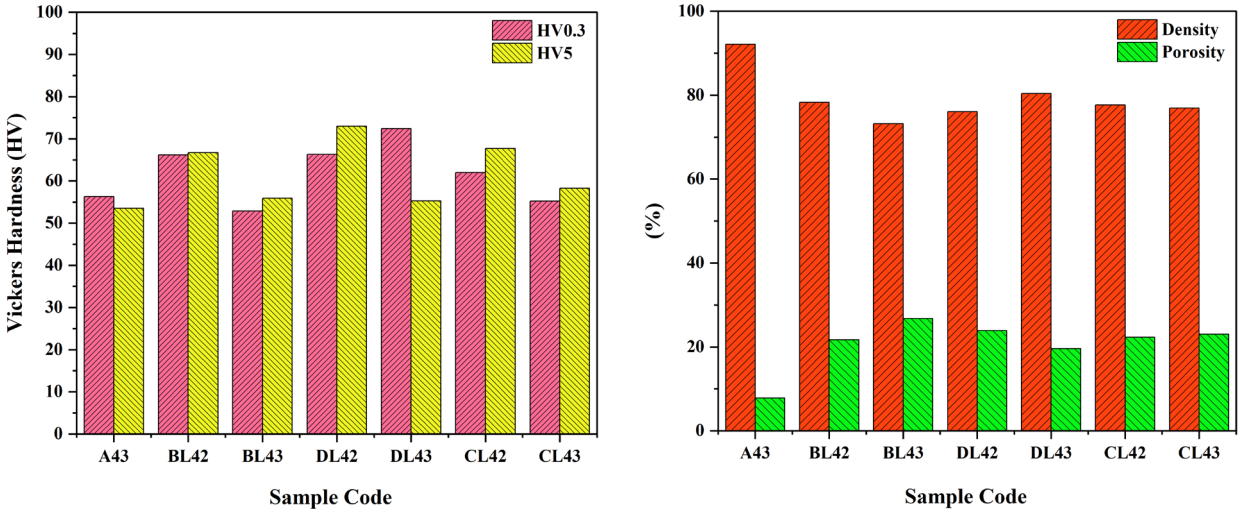

Fig. 5. The mechanical characteristic results of hot-pressed Zn-based nanocomposite samples.

3.3. Structural analysis

Fig. 6a–c shows the X-ray diffraction (XRD) analysis diagrams of the nanocomposite samples, which were conducted using a Bruker D8 Advance instrument. For the mentioned sample groups that hot-pressed at different temperatures revealed that they are fully compatible with the standard PDF cards – ICDD 01-077-1177, ICDD 00-006-0664, ICDD 01-074-9943, ICDD 00-030-0794, ICDD 00-027-0759, and ICDD 03-065-1853 exhibit distinct diffraction peaks corresponding to the crystallographic planes of zinc.

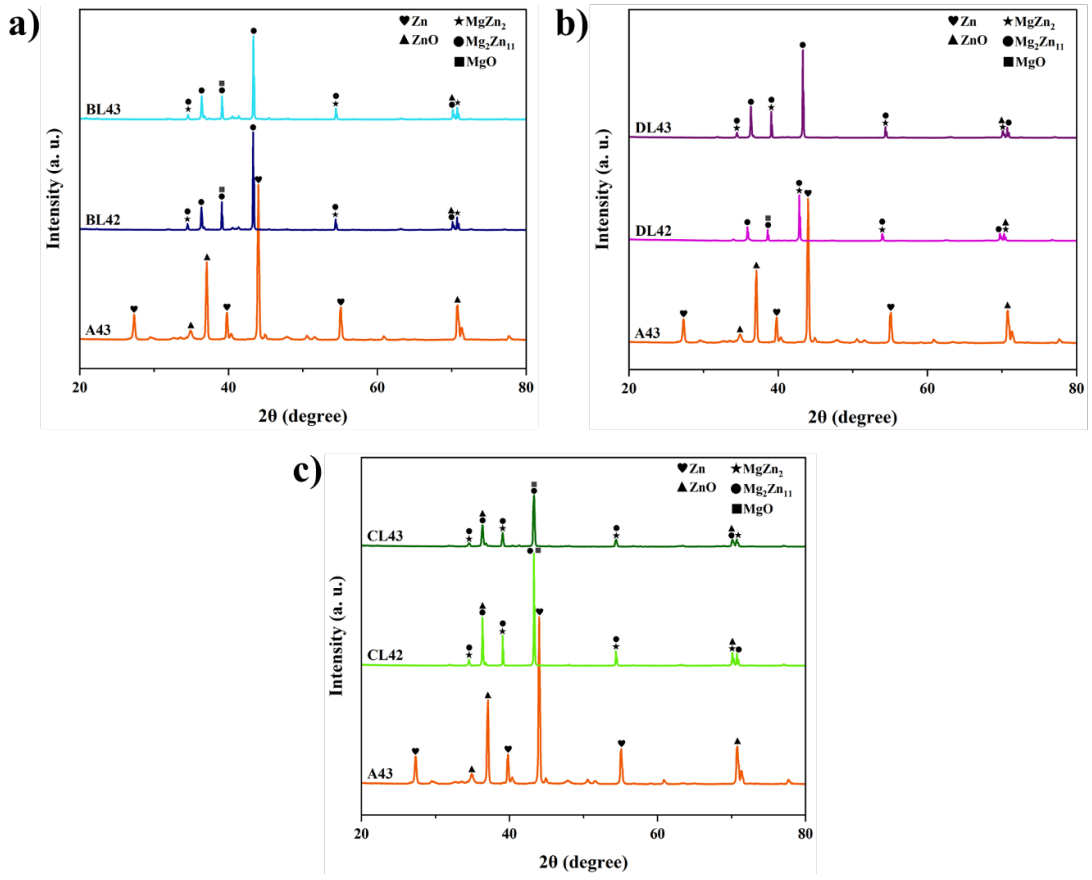

Fig. 6. a–c) The X-ray diffraction (XRD) analysis diagrams of Zn-based nanocomposite samples.

The reinforcement of pure Mg and various Mg alloy powders into the zinc matrix caused the pure zinc peaks to shift to the left on the XRD diagrams. Furthermore, the obtained XRD analysis results confirmed that both pure zinc (Zn) and zinc oxide (ZnO) have a hexagonal crystal structure, which are the primary matrix phases. Significant reflections of Zn were determined in the reference pure zinc sample at the (111), (100), (101), and (102) planes corresponding to two theta (2θ) angle values of 27.361 °, 39.802 °, 44.014 °, and 55.096 ° [36, 37]. Additionally, pronounced reflections were observed at the (002), (101), and (201) planes corresponding to two theta (2θ) angle values of 35.146 °, 36.926 °, and 70.464 °, respectively. These reflections supported by narrow and intense diffraction peaks in all three sample groups confirm the presence of crystalline ZnO phase alongside the structural consistency and various phase stability of the hot pressed nanocomposite materials.

In addition to the primary ZnO phase, the formation of intermetallic compounds containing zinc (Zn) and magnesium (Mg), especially $MgZn_2$ and Mg_2Zn_{11}, was identified. The $MgZn_2$ phase, characterized by its hexagonal crystal structure was confirmed by the reflections of the (110), (200), (004), (210), and (211) planes corresponding to two theta (2θ) angle values of 34.311 °, 39.826 °, 42.164 °, 53.560 °, and 54.704 °, respectively. Similarly, the presence of Mg_2Zn_{11} phase exhibiting cubic crystal structure was shown by prominent diffraction peaks in (311), (222), (321), (400), (410), (500), and (510) planes corresponding to two theta (2θ) angle values of 34.743 °, 36.343 °, 39.312 °, 42.195 °, 43.694 °, 53.547 °, and 54.759 °, respectively. In addition to these intermetallic phases, the presence of magnesium oxide (MgO) phase with cubic crystal structure observed in SEM micrographs was confirmed by (222) plane reflection corresponding to two theta (2θ) angle values of 38.439 °, respectively. The evaluated XRD results are in full agreement with the findings reported in the literature [28, 30, 31], and the presence of $MgZn_2$, Mg_2Zn_{11} and MgO phases was detected in addition to the Zn and ZnO primary matrix phase.

4. Conclusions

In this study, 10 wt% Mg, WE43 and AZ91 reinforced Zn based nanocomposites were successfully synthesized by powder metallurgy method, then the effects of 200 °C and 300 °C pressing temperatures under 400 MPa constant pressure on the microstructural and mechanical characteristics of the samples were investigated. The results obtained showed that increasing the pressing temperature and incorporating reinforcement powders enhanced density, hardness, and intermetallic phase formation. Samples processed at 300 °C exhibited superior mechanical integrity, with the formation of $MgZn_2$, Mg_2Zn_{11} and MgO phases affected the microstructural characteristics. The Vickers macro- and micro-hardness values range between 52.9 HV and 73.0 HV, depending on porosity and intermetallic distribution. Therefore, the nanocomposites hot pressed under 400 MPa pressure and 300 °C temperature demonstrated the most promising mechanical properties for implant applications, highlighting their potential suitability for biomedical use. Future research should focus on investigating biodegradation and corrosion resistance through in-vitro and in-vivo studies, as well as further optimizing processing parameters to enhance performance.

CRediT authorship contribution statement

Onur Fevzi Kevenlik: Investigation, Conceptualization, Methodology, Data curation, Project administration, Writing – original draft.
Shanli Salahi: Investigation, Conceptualization, Methodology, Data curation, Writing – original draft.
Yiğit Yalçın: Investigation, Methodology, Data curation.
Hanifi Çinici: Conceptualization, Data curation, Validation, Writing – review & editing.
Recep Çalın: Project administration, Supervision, Funding, Writing – review & editing.

Data availability

The data underlying this article will be shared on reasonable request to the corresponding author.

Declaration of competing interest

The authors declare no competing interests.

Funding and acknowledgment

We extend our gratitude to the Kırıkkale University Scientific Research Projects (KKÜ BAP) Unit for providing an academic grant under Project ID No. of 2023-072. Furthermore, the Metallurgical and Materials Engineering department of Gazi University is acknowledged for providing laboratory facilities.

References

[1] H. Hermawan, Biodegradable Metals: State of the Art, Springer, Berlin, Heidelberg. (2012) 13–22. https://doi.org/10.1007/978-3-642-31170-3_2.
[2] Y. Yun, Z. Dong, N. Lee, Y. Liu, D. Xue, et al., Revolutionizing biodegradable metals, Mater. Today. 12 (2009) 22–32. https://doi.org/10.1016/S1369-7021(09)70273-1.
[3] M. Moravej, D. Mantovani, Biodegradable Metals for Cardiovascular Stent Application: Interests and New Opportunities, Int. J. Mol. Sci. 12 (2011) 4250–4270. https://doi.org/10.3390/ijms12074250.
[4] H. Gong, J. Agustin, D. Wootton, J.G. Zhou, Biomimetic design and fabrication of porous chitosan–gelatin liver scaffolds with hierarchical channel network, J. Mater. Sci. Mater. Med. 25 (2014) 113–120. https://doi.org/10.1007/s10856-013-5061-8.
[5] P. Suomalainen, A.-S. Moisala, A. Paakkala, P. Kannus, T. Järvelä, Comparison of tunnel placements and clinical results of single-bundle anterior cruciate ligament reconstruction before and after starting the use of double-bundle technique, Knee Surgery, Sport. Traumatol. Arthrosc. 21 (2013) 646–653. https://doi.org/10.1007/s00167-012-1981-y.
[6] R. Hänsch, R.R. Mendel, Physiological functions of mineral micronutrients (Cu, Zn, Mn, Fe, Ni, Mo, B, Cl), Curr. Opin. Plant Biol. 12 (2009) 259–266. https://doi.org/10.1016/j.pbi.2009.05.006.
[7] H. Tapiero, K.D. Tew, Trace elements in human physiology and pathology: zinc and metallothioneins, Biomed. Pharmacother. 57 (2003) 399–411. https://doi.org/10.1016/S0753-3322(03)00081-7.
[8] D. Vojtěch, J. Kubásek, J. Šerák, P. Novák, Mechanical and corrosion properties of newly developed biodegradable Zn-based alloys for bone fixation, Acta Biomater. 7 (2011) 3515–3522. https://doi.org/10.1016/j.actbio.2011.05.008.

[9] L.M. Plum, L. Rink, H. Haase, The Essential Toxin: Impact of Zinc on Human Health, Int. J. Environ. Res. Public Health. 7 (2010) 1342–1365. https://doi.org/10.3390/ijerph7041342.
[10] H.F. Li, X.H. Xie, Y.F. Zheng, Y. Cong, F.Y. Zhou, et al., Development of biodegradable Zn-1X binary alloys with nutrient alloying elements Mg, Ca and Sr, Sci. Rep. 5 (2015) 10719. https://doi.org/10.1038/srep10719.
[11] H. Li, Y. Zheng, L. Qin, Progress of biodegradable metals, Prog. Nat. Sci. Mater. Int. 24 (2014) 414–422. https://doi.org/10.1016/j.pnsc.2014.08.014.
[12] P.K. Bowen, J. Drelich, J. Goldman, Zinc Exhibits Ideal Physiological Corrosion Behavior for Bioabsorbable Stents, Adv. Mater. 25 (2013) 2577–2582. https://doi.org/10.1002/adma.201300226.
[13] E.R. Shearier, P.K. Bowen, W. He, A. Drelich, J. Drelich, et al., In Vitro Cytotoxicity, Adhesion, and Proliferation of Human Vascular Cells Exposed to Zinc, ACS Biomater. Sci. Eng. 2 (2016) 634–642. https://doi.org/10.1021/acsbiomaterials.6b00035.
[14] P.K. Bowen, E.R. Shearier, S. Zhao, R.J. Guillory, F. Zhao, et al., Biodegradable Metals for Cardiovascular Stents: from Clinical Concerns to Recent Zn-Alloys, Adv. Healthc. Mater. 5 (2016) 1121−1140. https://doi.org/10.1002/adhm.201501019.
[15] E. Jablonská, D. Vojtěch, M. Fousová, J. Kubásek, J. Lipov, et al., Influence of surface pre-treatment on the cytocompatibility of a novel biodegradable ZnMg alloy, Mater. Sci. Eng. C. 68 (2016) 198–204. https://doi.org/10.1016/j.msec.2016.05.114.
[16] J. Kubásek, D. Vojtěch, E. Jablonská, I. Pospíšilová, J. Lipov, T. Ruml, Structure, mechanical characteristics and in vitro degradation, cytotoxicity, genotoxicity and mutagenicity of novel biodegradable Zn–Mg alloys, Mater. Sci. Eng. C. 58 (2016) 24–35. https://doi.org/10.1016/j.msec.2015.08.015.
[17] M.P. Staiger, A.M. Pietak, J. Huadmai, G. Dias, Magnesium and its alloys as orthopedic biomaterials: A review, Biomaterials. 27 (2006) 1728–1734. https://doi.org/10.1016/j.biomaterials.2005.10.003.
[18] F. Witte, N. Hort, C. Vogt, S. Cohen, K.U. Kainer, et al., Degradable biomaterials based on magnesium corrosion, Curr. Opin. Solid State Mater. Sci. 12 (2008) 63–72. https://doi.org/10.1016/j.cossms.2009.04.001.
[19] C.K. Seal, K. Vince, M.A. Hodgson, Biodegradable surgical implants based on magnesium alloys – A review of current research, IOP Conf. Ser. Mater. Sci. Eng. 4 (2009) 012011. https://doi.org/10.1088/1757-899X/4/1/012011.
[20] R. Zeng, W. Dietzel, F. Witte, N. Hort, C. Blawert, Progress and Challenge for Magnesium Alloys as Biomaterials, Adv. Eng. Mater. 10 (2008) B3–B14. https://doi.org/10.1002/adem.200800035.
[21] A. Krause, N. von der Höh, D. Bormann, C. Krause, F.-W. Bach, et al., Degradation behaviour and mechanical properties of magnesium implants in rabbit tibiae, J. Mater. Sci. 45 (2010) 624–632. https://doi.org/10.1007/s10853-009-3936-3.
[22] M.S. Dambatta, S. Izman, H. Hermawan, D. Kurniawan, Influence of Heat Treatment Cooling Mediums on the Degradation Property of Biodegradable Zn-3Mg Alloy, Adv. Mater. Res. 845 (2013) 7–11. https://doi.org/10.4028/www.scientific.net/AMR.845.7.
[23] D. Zhang, G. Shi, X. Zhao, F. Qi, Microstructure evolution and mechanical properties of Mg-x%Zn-1%Mn (x=4, 5, 6, 7, 8, 9) wrought magnesium alloys, Trans. Nonferrous Met. Soc. China. 21 (2011) 15–25. https://doi.org/10.1016/S1003-6326(11)60672-9.
[24] H. Li, H. Yang, Y. Zheng, F. Zhou, K. Qiu, X. Wang, Design and characterizations of novel biodegradable ternary Zn-based alloys with IIA nutrient alloying elements Mg, Ca and Sr, Mater. Des. 83 (2015) 95–102. https://doi.org/10.1016/j.matdes.2015.05.089.
[25] J. Čapek, E. Jablonská, J. Lipov, T.F. Kubatík, D. Vojtěch, Preparation and characterization of porous zinc prepared by spark plasma sintering as a material for biodegradable scaffolds, Mater. Chem. Phys. 203 (2018) 249–258. https://doi.org/10.1016/j.matchemphys.2017.10.008.
[26] X.N. Gu, W.R. Zhou, Y.F. Zheng, Y. Cheng, S.C. Wei, et al., Corrosion fatigue behaviors of two biomedical Mg alloys – AZ91D and WE43 – In simulated body fluid, Acta Biomater. 6 (2010) 4605–4613. https://doi.org/10.1016/j.actbio.2010.07.026.
[27] H. Gong, K. Wang, R. Strich, J.G. Zhou, In vitro biodegradation behavior, mechanical properties, and cytotoxicity of biodegradable Zn–Mg alloy, J. Biomed. Mater. Res. Part B Appl. Biomater. 103 (2015) 1632–1640. https://doi.org/10.1002/jbm.b.33341.
[28] S.A.M.Y. Kolawole, J.O. Aweda, F. Iqbal, A. Ali, Mechanical Properties of Powder Metallurgy Processed Biodegradable Zn-Based Alloy for Biomedical Application, Int. J. Mater. Metall. Eng. 13 (2019) 558–563. https://doi.org/10.5281/zenodo.3593236.
[29] T. Truglas, J. Duchoslav, C. Riener, M. Arndt, C. Commenda, et al., Correlative characterization of Zn-Al-Mg coatings by electron microscopy and FIB tomography, Mater. Charact. 166 (2020) 110407. https://doi.org/10.1016/j.matchar.2020.110407.
[30] Y. Zhang, Q. Li, T. Guo, S. Li, Effect of Y Content on Properties of Extruded Zn-1.5Mg-xY Alloys for Medical Applications, Mater. Res. 22 (2019) e20190004. https://doi.org/10.1590/1980-5373-mr-2019-0004.
[31] P. Gogola, Z. Gabalcová, M. Kusý, H. Suchánek, The Effect of Sn Addition on Zn-Al-Mg Alloy; Part I: Microstructure and Phase Composition, Materials (Basel). 14 (2021) 5404. https://doi.org/10.3390/ma14185404.
[32] U. Tasci, T.A. Yilmaz, B. Bostan, Investigation of microstructure, wear and transverse rupture strength of WE43/nano B4C composites produced by powder metallurgy method, Tribol. Int. 180 (2023) 108231. https://doi.org/10.1016/j.triboint.2023.108231.
[33] C. Gül, S. Albayrak, H. Çinici, Characterization of Tantalum Oxide Sol–Gel-coated AZ91 Mg Alloys, Trans. Indian Inst. Met. 73 (2020) 1249–1256. https://doi.org/10.1007/s12666-020-01976-y.
[34] H. Yang, B. Jia, Z. Zhang, X. Qu, G. Li, et al., Alloying design of biodegradable zinc as promising bone implants for load-bearing applications, Nat. Commun. 11 (2020) 401. https://doi.org/10.1038/s41467-019-14153-7.
[35] I. Pospíšilová, D. Vojtěch, Zinc Alloys for Biodegradable Medical Implants, Mater. Sci. Forum 782 (2014) 457–460. https://doi.org/10.4028/www.scientific.net/MSF.782.457.
[36] J. Madhavi, Comparison of average crystallite size by X-ray peak broadening and Williamson–Hall and size–strain plots for VO2+ doped ZnS/CdS composite nanopowder, SN Appl. Sci. 1 (2019) 1509. https://doi.org/10.1007/s42452-019-1291-9.
[37] H. Li, J. Huang, P. Zhang, Q. Zhang, Investigation on tribological behaviors of biodegradable pure Zn and Zn-X (Li, Cu, Ge) binary alloys, J. Mater. Sci. Mater. Med. 32 (2021) 149. https://doi.org/10.1007/s10856-021-06625-4.